



RESEARCH ACTIVITIES

Theoretical and Computational Molecular Science

It is our goal to develop new theoretical and computational methods based on quantum mechanics, statistical mechanics, and molecular simulation in order to predict and understand the structures, reactions, and functions of molecules in gas, solution, and condensed phases as well as in nano- and bio-systems prior to or in cooperation with experiment.

Theoretical Study and Design of Functional Molecules: New Bonding, Structures, and Reactions

Department of Theoretical and Computational Molecular Science
Division of Theoretical Molecular Science I



NAGASE, Shigeru
OHTSUKA, Yuki
TANAKA, Masato
KATOUDA, Michio
GAO, Xingfa
GUO, Jing-Doing
WANG, Lu
MIYAKE, Toshiko
LUO, Gangfu
GHOSH, Manik Kumer
WATANABE, Hidekazu
SAKAKI, Shigeyoshi
YAMADA, Mariko
KONDO, Naoko

Professor
Assistant Professor
IMS Fellow
Post-Doctoral Fellow
Post-Doctoral Fellow*
Post-Doctoral Fellow
Post-Doctoral Fellow†
Post-Doctoral Fellow‡
Post-Doctoral Fellow
Post-Doctoral Fellow
Post-Doctoral Fellow
Visiting Scientist
Secretary
Secretary

In theoretical and computational chemistry, it is an important goal to develop functional molecules prior to or in cooperation with experiment. Thus, new bonds and structures provided by heavier atoms are investigated together with the reactivities. In addition, chemical modification and properties of nanocarbons are investigated to develop functional nanomolecular systems. Efficient computational methods are also developed to perform reliable quantum chemistry calculations for small and large molecular systems.

1. Application of Second-Order Møller-Plesset Perturbation Theory with Resolution-of-Identity Approximation to Periodic Systems

Electron correlation plays an important role in the accurate description of the conductive, optical, and magnetic properties of periodic systems. Second-order Møller-Plesset perturbation theory (MP2) is the simplest method to account for electron correlation at an *ab initio* level. Periodic boundary condition (PBC) calculations by the MP2 method (PBC MP2) have been developed. However, the computational cost is considerably high and practical applications are limited to small periodic systems. A promising approach to reduce the computational cost is resorting to the resolution-of-identity (RI) approximation of four-center two-electron atomic integrals (ERIs). However, no attempt has been made to incorporate the RI approximation with the PBC MP2 method because the lattice sums of long-range AO ERIs show extremely slow r^{-1} decay.

Therefore, we have developed an efficient PBC RI-MP2 method in the crystal orbital framework, which is applicable to large periodic systems.¹⁾ In this method, the slow convergence of lattice sum of long-range AO ERIs is avoided using Poisson and Gaussian mixed auxiliary basis functions. To assess the accuracy and computational efficiency of the developed PBC RI-MP2 code, test calculations were performed for trans-polyacetylene using the 6-31G** basis sets. PBC RI-MP2 is

98 times faster than PBC MP2, and the energy difference between PBC RI-MP2 and PBC MP2 is only 0.4 mH. In addition, the required memory and disk sizes for PBC RI-MP2 are much smaller than those for PBC MP2. To calculate much larger periodic systems, we plan to develop an efficient parallel code of PBC RI-MP2.

2. Molecular Tailoring Approach to Very Large Molecules

Several divide-and-conquer approaches have been developed to overcome the high scaling problem of *ab initio* calculations. The molecular tailoring approach (MTA) was interfaced with the efficient MP2 and RI-MP2 codes developed in our group.^{2,3)} The performance was extensively benchmarked for a variety of large molecular systems and critically compared with the popular fragment molecular orbital (FMO) method. It was found that FMO2-MP2 is superior to FMO3-MP2 and MTA-MP2 in terms of computational costs. However, the errors of FMO2-MP2 are considerably large and beyond chemical accuracy. FMO3-MP2 is accurate for biological systems, while it is unsuccessful for water clusters. The errors of MTA-MP2 are within 1 kcal/mol for all systems with reasonable time advantage. The accuracy of FMO decreases for the basis sets that include diffuse functions. In contrast, MTA performs well regardless of basis sets.

3. Application of Projector Monte Carlo Method Based on Slater Determinants to Excited States

A projector Monte Carlo method based on Slater determinants (PMC-SD) is expanded to excited state calculations.⁴⁾ Target excited states are calculated state-by-state by eliminating the components of the lower states from the imaginary time propagator. As the test calculations of excited states of

H₂O show, the accuracy of the PMC-SD method is improved systematically by increasing the number of walkers and the full-CI energies are obtainable as a limit for a given basis set. The avoided crossing of covalent and ionic states in the dissociation of LiF is well reproduced using the PMC-SD method.

4. New Bonds Provided by Heavier Main Group Elements and Functionalization of Endohedral Metallofullerenes and Nanographenes

Silicon behaves like carbon in forming covalent bonds to four neighboring atoms. These bonds form the framework of many organosilicon compounds and crystalline silicon. Silicon can also form a pentacoordinated anionic structure, a so-called silicate. No compounds containing a direct bond between two silicate moieties (disilicates), where two silicate structures are combined in one species, have been reported because of the electronic repulsion between the anionic halves and difficulty preventing the release of anions. However, we have developed a stable compound containing the linkage of two pentavalent silicon atoms, as shown in Figure 1.⁵⁾ The unique electronic properties are promising for the construction of functional materials with silicon wire made up of silicate chains.

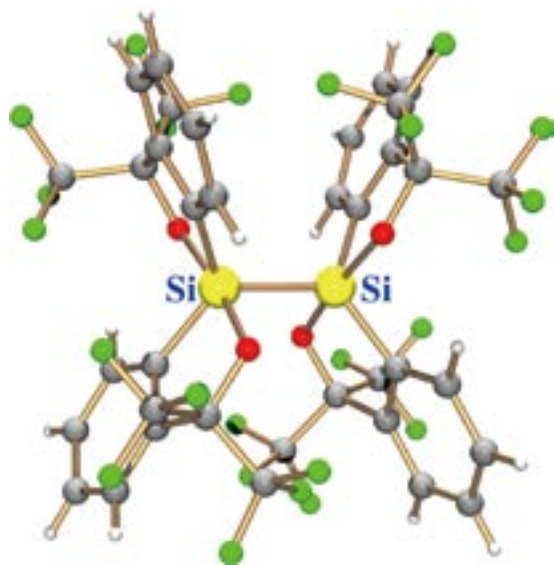


Figure 1. The stable bond between pentavalent silicon atoms.

The concept of aromaticity has long played an important role in carbon chemistry since the discovery of benzene in 1825. To determine that the heavier group 14 elements can sustain aromaticity, silicon, germanium, and tin analogs of carbocyclic aromatic compounds have been synthesized, most of these showing considerable aromaticity. However, there has

been no clear evidence of whether the concept of aromaticity can be expanded to the ring incorporating the heaviest lead atom. Very recently, dilithioplumbole has been successfully synthesized and isolated in collaboration with our research group.⁶⁾ Relativistic theoretical calculations show that its cyclic compound has considerable aromatic character as a result of the important overlap between 2p (C) and 6p (Pb) orbitals. The present results highlight the future possibility of introducing heavier elements including Pb into a broader range of carbon frameworks.

Chemical functionalization of endohedral metallofullerenes regulates the positions and movements of the encapsulated metal atoms.⁷⁾ This control of metal positions and movements within fullerene cages can be valuable for designing functional molecular devices with new electronic or magnetic properties. Also investigated are graphene oxides and monovalency defects in graphene.^{8,9)}

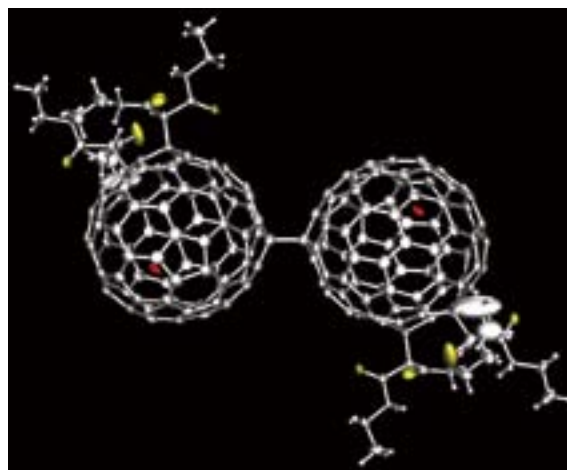


Figure 2. Functionalization of endohedral metallofullerenes.

References

- 1) M. Katouda and S. Nagase, *J. Chem. Phys.* **133**, 184103 (9 pages) (2010).
- 2) M. Katouda and S. Nagase, *Int. J. Quant. Chem.* **109**, 2121–2130 (2009).
- 3) A. P. Rahalkar, M. Katouda, S. R. Gadre and S. Nagase. *J. Comput. Chem.* **31**, 2405–2418 (2010).
- 4) Y. Ohtsuka and S. Nagase, *Chem. Phys. Lett.* **485**, 367–370 (2010).
- 5) N. Kano, H. Miyake, K. Sasaki, T. Kawashima, N. Mizorogi and S. Nagase, *Nat. Chem.* **2**, 112–116 (2010).
- 6) M. Saito, M. Sakaguchi, T. Tajima, K. Ishimura, S. Nagase and M. Hada, *Science* **328**, 339–342 (2010).
- 7) M. Yamada, T. Akasaka and S. Nagase, *Acc. Chem. Res.* **43**, 92–102 (2010).
- 8) X. Gao, J. Jiang and S. Nagase, *J. Phys. Chem. C* **114**, 832–842 (2010).
- 9) X. Gao, L. Liu, S. Irlle and S. Nagase, *Angew. Chem., Int. Ed.* **49**, 3200–3202 (2010).

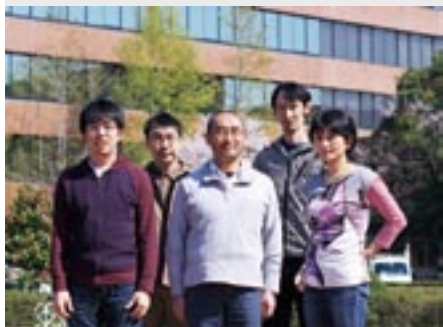
* Present Address; Department of Physics and Applied Physics, Research Polytechnic Institute, New York 12180, U.S.A.

† Present Address; Department of Physics, University of Nebraska at Omaha, Nebraska 68182-0266, U.S.A.

‡ Present Address; Department of Chemistry, Hiroshima University, Higashi-Hiroshima 739-8526

Electron and Electromagnetic Field Dynamics in Nanostructures

Department of Theoretical and Computational Molecular Science
Division of Theoretical Molecular Science I



NOBUSADA, Katsuyuki
YASUIKE, Tomokazu
IWASA, Takeshi
KUBOTA, Yoji
NODA, Masashi
YAMADA, Mariko

Associate Professor
Assistant Professor
JSPS Post-Doctoral Fellow
Post-Doctoral Fellow
Post-Doctoral Fellow
Secretary

We have developed theoretical methods to calculate photo-induced electron dynamics in nanostructured materials such as nanoparticles, quantum-dot arrays, and adsorbate-surface systems. Specifically, we have developed generalized theory of a light-matter interaction beyond a dipole approximation on the basis of the multipolar Hamiltonian with the aim of understanding the near-field excitation of molecules at the 1 nm scale. Optical forces exerted on a 1 nm-sized metal particle were calculated in the framework of real-time and real-space time-dependent density functional theory combined with the new light-matter interaction formalism. We have also studied exciton-polariton transmission in quantum dot waveguides in an array of quantum dot. Furthermore, collectivity of plasmonic excitations in small sodium clusters was investigated in depth.

1. Near-Field Induced Optical Force on a Metal Particle and C_{60} : Real Time and Real Space Electron Dynamics Simulation¹⁾

Optical forces induced by a near-field are calculated for a 1 nm-sized metal particle mimicked by a jellium model and for C_{60} in the framework of real-time and real-space time-dependent density functional theory combined with a non-uniform light-matter interaction formalism, fully taking account of multipole interaction. A highly localized near-field non-uniformly polarizes these molecules. The locally induced polarization charges in the molecules are partly canceled by the screening charges. The polarization and screening charges generally contribute to the attractive and repulsive forces, respectively, and a sensible balance between these charges results in several peaks in the optical force as a function of the frequency of the near-field. The resonance excitation does not necessarily maximally induce the net force and the force exerted on the molecules strongly depends on the details of their electronic structures. The optical force is larger in the metal particle than C_{60} . We also found that the optical force depends linearly on the intensity of the near-field.

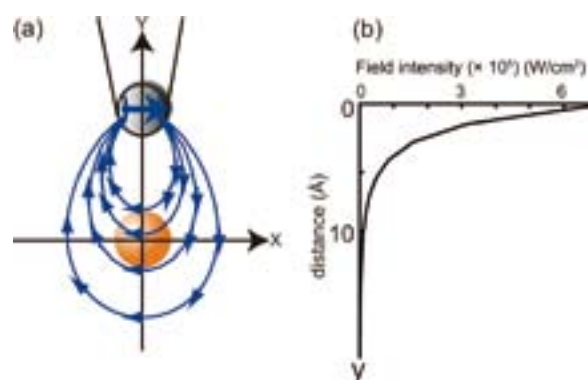


Figure 1. (a) Schematic of a near-field fiber tip (gray ball) and a target particle (orange ball). The near-field is approximated by the radiation from an x -polarized oscillating dipole (solid blue arrow). The blue curves denote the electric field lines. (b) Electric field intensity as a function of distance between the tip and the particle.

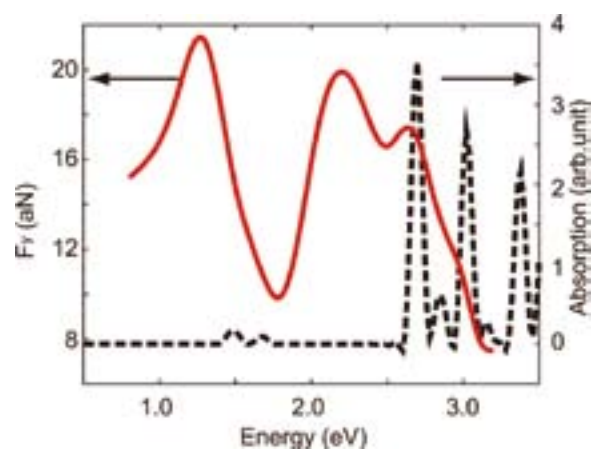


Figure 2. Absorption spectrum (dashed-black) of the silver nanoparticle and the time-averaged force on the particle (red) as a function of energy.

2. Exciton–Polariton Transmission in Quantum Dot Waveguides and a New Transmission Path due to Thermal Relaxation²⁾

Exciton–polariton transmission in quantum dot waveguides is investigated with quantum time-evolution equations in Liouville space for quantum wave packet dynamics. The transmission efficiency of the exciton–polariton wave with the longitudinal and transverse mode transformation strongly depends on the geometric parameters (bending angle and interdot distance) of the waveguides and on configuration of an additional branch attached to the waveguide. We have numerically demonstrated the transmission efficiency significantly improves by controlling these geometric parameters and the configuration of the branched waveguide. The optimal bending angle for efficient transmission with the longitudinal and transverse mode transformation deviates from the right angle owing to more than nearest-neighbor-site interactions through a shortcut. We have also found that existence of thermal relaxation enables to open a new transmission channel along which the exciton–polariton transmission through the Coulomb interaction is suppressed.

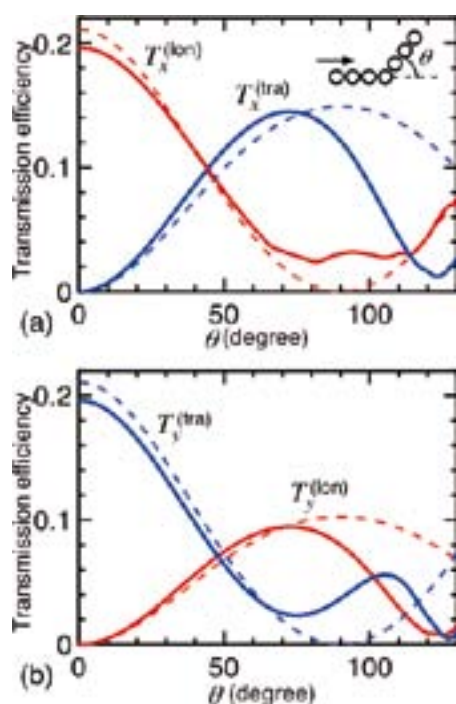


Figure 3. Bending angle dependence of transmission efficiency. The solid and dashed curves are the results for the full interaction calculations and for the calculation under the nearest-neighbor interaction approximation, respectively.

3. Collectivity of Plasmonic Excitations in Small Sodium Clusters

Plasmonic excitations in small sodium clusters are investi-

gated by using the linear-response density functional theory (LRDFT). The computed photoabsorption spectra show a small number of strong peaks, and the intensities for some of those peaks monotonically grow up with increasing the cluster size. The dipolar character of the transition density distributions for them shows a clear correspondence to a classical picture of plasmonic excitation. The collectivity of the electronic motion induced by the plasmonic excitation is quantitatively analyzed in terms of the collectivity index defined by the transition density matrix. The excitation mode dependence of the collectivity in non-spherical clusters and large collectivities for the higher-energy plasmonic excitations are found. The collectivity analysis also clarifies the existence of the non-dipolar collective motion at the energies very close to the higher-energy plasmonic excitations. The importance of the non-dipolar motion is pointed out in light of nano-optics.

4. Isolation, Structure, and Stability of a Dodecanethiolate-Protected Pd₁Au₂₄ Cluster³⁾

A dodecanethiolate-protected Pd₁Au₂₄(SC₁₂H₂₅)₁₈ cluster, which is a mono-Pd-doped cluster of the well understood magic gold cluster Au₂₅(SR)₁₈, was isolated in high purity using solvent fractionation and high-performance liquid chromatography (HPLC) after the preparation of dodecanethiolate-protected palladium–gold bimetal clusters. The cluster thus isolated was identified as the neutral [Pd₁Au₂₄(SC₁₂H₂₅)₁₈]⁰ from the retention time in reverse phase columns and by elemental analyses. The LDI mass spectrum of [Pd₁Au₂₄(SC₁₂H₂₅)₁₈]⁰ indicates that [Pd₁Au₂₄(SC₁₂H₂₅)₁₈]⁰ adopts a similar framework structure to Au₂₅(SR)₁₈, in which an icosahedral Au¹³ core is protected by six [–S–Au–S–Au–S–] oligomers. The optical absorption spectrum of [Pd₁Au₂₄(SC₁₂H₂₅)₁₈]⁰ exhibits peaks at ~690 and ~620 nm, which is consistent with calculated results on [Pd₁@Au₂₄(SC₁H₃)₁₈]⁰ in which the central gold atom of Au₂₅(SC₁H₃)₁₈ is replaced with Pd. These results strongly indicate that the isolated [Pd₁Au₂₄(SC₁₂H₂₅)₁₈]⁰ has a core-shell [Pd₁@Au₂₄(SC₁₂H₂₅)₁₈]⁰ structure in which the central Pd atom is surrounded by a frame of Au₂₄(SC₁₂H₂₅)₁₈. Experiments on the stability of the cluster showed that Pd₁@Au₂₄(SC₁₂H₂₅)₁₈ is more stable against degradation in solution and laser dissociation than Au₂₅(SC₁₂H₂₅)₁₈. These results indicate that the doping of a central atom is a powerful method to increase the stability beyond the Au₂₅(SR)₁₈ cluster.

References

- 1) T. Iwasa and K. Nobusada, *Phys. Rev. A* **80**, 043409 (11 pages) (2009).
- 2) Y. Kubota and K. Nobusada, *J. Phys. Soc. Jpn.* **78**, 114603 (7 pages) (2009).
- 3) Y. Negishi, W. Kurashige, Y. Niihori, T. Iwasa and K. Nobusada, *Phys. Chem. Chem. Phys.* **12**, 6219–6225 (2010).

Advanced Electronic Structure Theory in Quantum Chemistry

Department of Theoretical and Computational Molecular Science
Division of Theoretical Molecular Science I



YANAI, Takeshi
KURASHIGE, Yuki
MIZUKAMI, Wataru
YAMADA, Mariko

Associate Professor
Assistant Professor
Graduate Student
Secretary

Aiming at predictive computational modelings of molecular electronic structures with *ab initio* quantum chemistry calculations, our scientific exploration is to establish a cutting-edge theoretical methodology that allows one to compute accurately and efficiently the complex electronic structures, in which strongly-interacting electrons play a crucial role to characterize the nature of molecules. The complicated electronic structures can be handled accurately with the multi-reference theory, which deals with multiple important electronic configurations on equal footing. However, with the standard multireference methods such as the complete active space self-consistent field (CASSCF), the tractable size of the reference space is limited to small active space because the complexity of the calculations grows exponentially with the reference size. The existing multireference methods are nevertheless usefully applied to chemical theory problems such as exploring chemical reactions of bonding, dissociation and isomerization along the reaction coordinates, electronically excited states, unstable electronic structures of radical systems, and multiple covalent bindings in molecular metal complexes, *etc.* Our resultant works to be reported here are (1) to develop a type of the multireference correlation model named Canonical Transformation (CT) theory, which can efficiently describe short-range dynamic correlation on top of the multi-configurational starting wave function, and (2) to construct the extensive complete active space self-consistent field (CASSCF) method combined with *ab initio* density matrix renormalization group (DMRG) method for making unprecedentedly larger active spaces available for the CASSCF calculations.

1. Discovery of New Quantum States of Electron Spins in Polycarbenes from *Ab Initio* Density Matrix Renormalization Group Calculations¹⁾

An investigation into spin structures of poly(*m*-phenylene-carbene)s, a prototype of organic magnetic molecules, is presented using the *ab initio* density matrix renormalization group method. It is revealed by achieving large-scale multi-

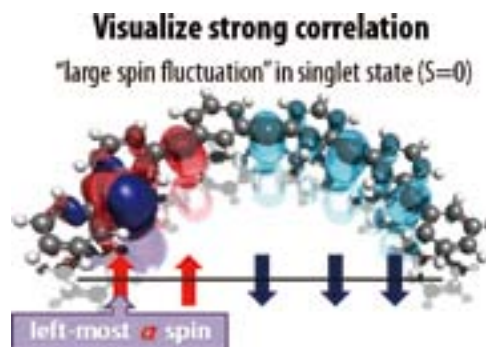


Figure 1. The spin correlation densities $\sigma_i^{\text{spin}}(r)$ of the CASSCF wave functions with respect to the non-bonding sp^2 orbital on the leftmost carbene site of polycarbene with $n = 5$ (solid red and blue color) for the singlet state. Crystal red and blue represent α spin ($\sigma_i^{\text{spin}}(r) > 0$) and β spin ($\sigma_i^{\text{spin}}(r) < 0$), respectively. The density visualizes the spin correlation against the α spin at the nonbonding orbital at the leftmost carbene site. The orbital and molecular geometry is superimposed.

reference calculations that the energy differences between high-spin and low-spin states (spin-gaps) of polycarbenes decrease with increasing the number of carbene sites. This size-dependency of the spin-gaps strikingly contradicts the predictions with single-reference methods including density functional theory. The wave function analysis shows that the low-spin states are beyond the *classical* spin picture, namely, much of multireference character, and thus are manifested as strongly correlated *quantum* states. The size dependence of the spin-gaps involves an odd-even oscillation, which cannot be explained by the model Hamiltonians with a single magnetic-coupling constant (**Figure 1**).

2. Multireference Quantum Chemistry through a Joint Density Matrix Renormalization Group and Canonical Transformation Theory²⁻⁴⁾

We presented the joint application of the density matrix

renormalisation group and canonical transformation theory to multireference quantum chemistry. The density matrix renormalization group provides the ability to describe static correlation in large active spaces, while the canonical transformation theory provides a high-order description of the dynamic correlation effects. We demonstrate the joint theory in two benchmark systems designed to test the dynamic and static correlation capabilities of the methods, namely (i) total correlation energies in long polyenes, and (ii) the isomerisation curve of the $[\text{Cu}_2\text{O}_2]^{2+}$ core. The largest complete active spaces treated by the joint DMRG-CT theory in these systems correspond to a (24e,24o) active space in the polyenes and a (28e,32o) active space in $[\text{Cu}_2\text{O}_2]^{2+}$.

3. *Ab Initio* Study of the Excited Singlet States of All-*trans* α,ω -Diphenylpolyenes with One to Seven Polyene Double Bonds: Simulation of the Spectral Data within Franck–Condon Approximation⁵⁾

Computational simulations of the electronic spectra with *ab initio* electronic structure calculations are presented for all-*trans* α,ω -diphenylpolyenes with the polyene double bond number (N) from one to seven. A direct comparison of the fluorescence spectra of diphenylpolyenes was made between the results of highly accurate calculations and the experimental data for the systems with various chain lengths. For the realistic simulation of the emission, the total vibrational wave function was described approximately as a direct product of one-dimensional (1D) vibrational wave functions along the normal coordinates that are determined from the vibrational analysis of the ground state. The observed spectra can be reproduced in a computationally efficient way by selecting effective C–C and C=C stretching modes for the constructions of the 1D vibrational Hamiltonians. The electronic structure

calculations were performed using the multireference Møller–Plesset perturbation theory with complete active space configuration interaction reference functions (CASCI-MRMP). Based on the vertical excitation energies computed, the lowest singlet excited state of diphenylbutadiene is shown to be the optically forbidden 2^1A_g state. The simulations of fluorescence spectra involving vibronic coupling effects reveal that the observed strong single C=C band consists of two major degenerate vibrational C=C modes for the shorter diphenylpolyenes with $N = 3$ and 5. Further, the relative intensities of the C–C stretching modes in the fluorescence spectra tend to be larger than those of the C=C stretching modes for the systems with N over 5. This indicates that the geometric differences of the energy minima between the ground (1^1A_g) and 2^1A_g states grows larger towards the direction of the C–C stretching mode with increasing N (Figure 2).

4. Tensor Factorizations of Local Second-Order Møller–Plesset Theory⁶⁾

Efficient electronic structure methods require efficient tensor representations of the wavefunction. Here we describe a general way to view tensor factorization. We use these ideas to construct low-complexity representations of the doubles amplitudes in local second order Møller–Plesset perturbation theory. We introduce two approximations—the direct factorized virtual approximation and the complete factorized virtual approximation. Conceptually, these lie between the projected atomic orbital representation used in the Pulay-Saebo local correlation theories and pair natural orbital correlation theories. We have tested the factorized virtual approximations on a variety of systems and properties including total energies, reaction energies, and potential energy curves. Compared to the Pulay-Saebo ansatz, we find that these approximations exhibit favourable accuracy and computational timings, while yielding smooth potential energy curves.

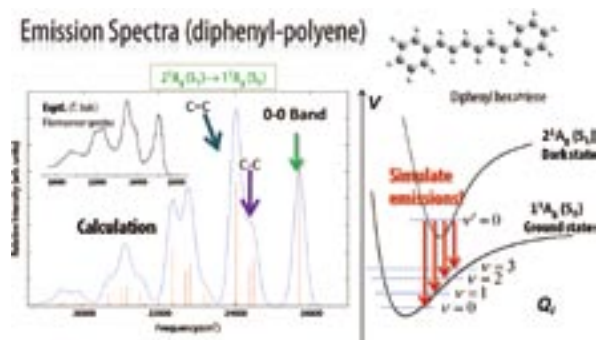


Figure 2. Simulated fluorescence spectrum of the vibronic transitions $2\text{A}_g \rightarrow 1\text{A}_g$ of all-*trans* α,ω -diphenylhexatriene (DP3) with $N = 3$ (N is the number of double bond in the polyene chain). Inset: The observed spectrum measured by T. Itoh (the Joint Studies Program (2008–2009) of the Institute for Molecular Science).

References

- 1) W. Mizukami, Y. Kurashige and T. Yanai, *J. Chem. Phys.* in press.
- 2) T. Yanai, Y. Kurashige, E. Neuscamman and G. K.-L. Chan, *J. Chem. Phys.* **132**, 024105 (9 pages) (2010).
- 3) E. Neuscamman, T. Yanai and G. K.-L. Chan, *J. Chem. Phys.* **132**, 024106 (13 pages) (2010).
- 4) E. Neuscamman, T. Yanai and G. K.-L. Chan, *Int. Rev. Phys. Chem.* **29**, 231 (2010).
- 5) W. Mizukami, Y. Kurashige, M. Ehara, T. Yanai and T. Itoh, *J. Chem. Phys.* **131**, 174313 (10 pages) (2009).
- 6) J. Yang, Y. Kurashige, F. R. Manby and G. K.-L. Chan, *J. Chem. Phys.*, submitted.

Award

MIZUKAMI, Wataru; 2009 The Best Poster Award at the 3rd annual meeting of Japan Society for Molecular Science.

Developing the Statistical Mechanics Theory of Liquids in Chemistry and Biophysics

Department of Theoretical and Computational Molecular Science
Division of Theoretical Molecular Science II



HIRATA, Fumio	Professor
CHONG, Song-ho	Assistant Professor
YOSHIDA, Norio	Assistant Professor
MARUYAMA, Yutaka	Post-Doctoral Fellow
MIYATA, Tatsuhiko	Post-Doctoral Fellow
PHONGPHANPHANEE, Saree	Post-Doctoral Fellow
SINDHIKARA, Daniel	Post-Doctoral Fellow
KIYOTA, Yasuomi	Graduate Student
SUETAKE, Yasumi	Secretary
KONDO, Naoko	Secretary
YAMADA, Mariko	Secretary

“Molecular recognition” is an essential elementary process for protein to function. The process is a thermodynamic process which is characterized with the free energy difference between two states of a host-guest system, namely, associated and dissociated states. It is readily understood that the structural fluctuation of protein gives a big effect on the free energy barrier. In that respect, the “molecular recognition” is a thermodynamic process which is conjugated with the structural fluctuation of protein.

We have been developing a new theory concerning the molecular recognition, based on the 3D-RISM/RISM theory which is a statistical mechanics of liquids. The theory has successfully “probed” small ligands such as water molecules and ions bound in a small cavity of protein.¹⁻³⁾

1. Ligand Mapping on Protein Surfaces by the 3D-RISM Theory: Toward Computational Fragment-Based Drug Design⁴⁾

In line with the recent development of fragment-based drug design, a novel computational method for mapping of small ligand molecules onto protein surface is proposed in this paper. The method uses the three-dimensional (3D) spatial distribution functions of the atomic sites of ligand calculated by a molecular theory of solvation, known as the 3D reference interaction site model (3D-RISM) theory, to identify the most probable binding modes of the ligand molecule. In this study, the 3D-RISM-based method is applied to the binding of several small organic solvents to thermolysin, in order to evaluate its efficiency. The results demonstrate that our method can reproduce the major binding modes found by X-ray crystallography with sufficient accuracy. Moreover, it is found that the method can successfully identify some binding modes associated with a known inhibitor, which could not be detected by the experiment. The dependence of ligand-binding modes on the ligand concentration, which can hardly be treated with other existing methods, is also investigated. The results indicate that some binding modes are readily affected by a shift in

the ligand concentration, while the others are not substantially altered. An analysis of the water distribution implies that the ligand-binding modes are determined by a subtle balance in the binding affinity between ligand and water.

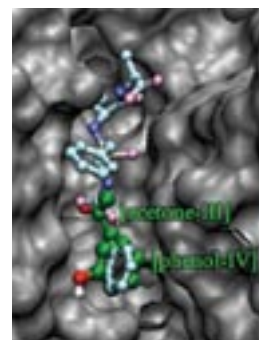


Figure 1. Comparison of two binding modes identified using 3D-RISM with the crystallographic structure in active site.

2. Molecular Selectivity in Aquaporin Channels Studied by the 3D-RISM Theory⁵⁾

The three dimensional distribution function (3D-DF) and potential of means force (PMF) of small neutral molecules inside the two aquaporin channels, AQP1 and GlpF, are calculated based on the 3D-RISM theory, the statistical mechanics theory of molecular liquids, in order to investigate the permeability of those ligands through the channels. The ligands investigated are Neon (Ne), carbon dioxide (CO₂), Nitrogen oxide (NO), ammonia (NH₃), urea, and glycerol.

Neon showed continuous distribution through out the channel pore in AQP1 as is the case of water, although the PMF of Ne at the selective filter (SF) region is higher than that of water, indicating that the stability of molecules in the channel is determined not only by their size, but also by the charge distribution. The ligand molecules, CO₂, NO, urea, and glycerol have large barrier in PMF at the SF region in AQP1, indicating that those ligands are not permeable through the

channel. On the other hand, NH_3 has only small activation barrier, ~ 2.5 kJ/mol, to be overcome. Therefore, our theory predicts that a NH_3 molecule can be permeated through the AQP1 channel. In GlpF, all the ligands have negative PMF throughout the channel except for glycerol which has a small barrier at the SF area, ~ 2.1 kJ/mol. The barrier can be readily overcome by the thermal motion. So, our results are quite consistent with the experiments for urea and glycerol, for which the corresponding data are available.

The potential of mean forces of the ligand molecules in GlpF obtained from the MD simulations show distinctly different patterns from our results: PMFs of NH_3 and urea from MD have large positive values throughout the channel, while those of CO_2 and glycerol has some negative regions. In any case, the barriers in PMF at the SF region are so high and large for all the four ligands examined. It seems impossible for them to overcome the barrier in order to be permeated through the channel. This raises a serious question to the results from MD simulations, because the experimental observation indicates that GlpF can conduct glycerol and urea pretty well. (Actually, the name “glyceroporin,” came from that function of the channel.)

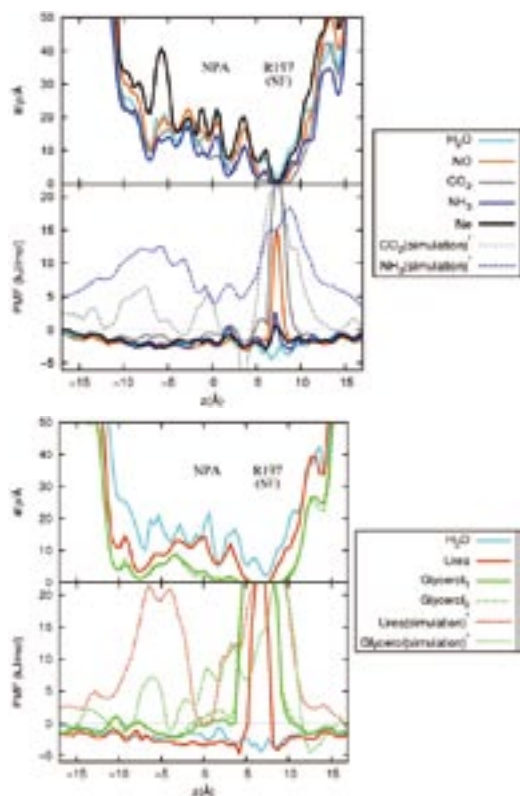


Figure 2. PMFs of water, Ne, CO_2 , NH_3 , urea and glycerol in AQP1.

3. Proton Transport through the Influenza A M2 Channel: 3D-RISM Study⁶⁾

The three dimensional distribution and the potential of mean force of water and hydronium ions in five protonated states of the Influenza A M2 channel are calculated by means

of the 3D-RISM theory in order to clarify the proton conduction mechanism of the channel. Each protonated state denoted as $i\text{H}$, where i runs from 0 to 4, has a different number of protonated histidines from 0 to 4. The distribution of water in each state exhibits closed structure of 0H, 1H and 2H, and opened structure in 3H and 4H. In the closed form, the distribution function and potential of mean forces calculated by the 3D-RISM theory indicate that hydronium ions are excluded from the channel. In contrast, the ion can distribute throughout the opened channel. The barrier in potential of mean force of 3H, ~ 3 –5 kJ/mol, is lower than that of 4H, 5–7 kJ/mol, indicating that 3H has higher permeability to proton. Based on the radial distribution functions of water and hydronium ions around the imidazole rings of His37, we propose a new mechanism of proton transfer through the gating region of the channel. In this process, a hydronium ion hands a proton to a non-protonated histidine through a hydrogen-bond between them, and then the other protonated histidine releases a proton to a water molecule via a hydrogen-bond. The process transfers a proton effectively from a water molecule to the other.

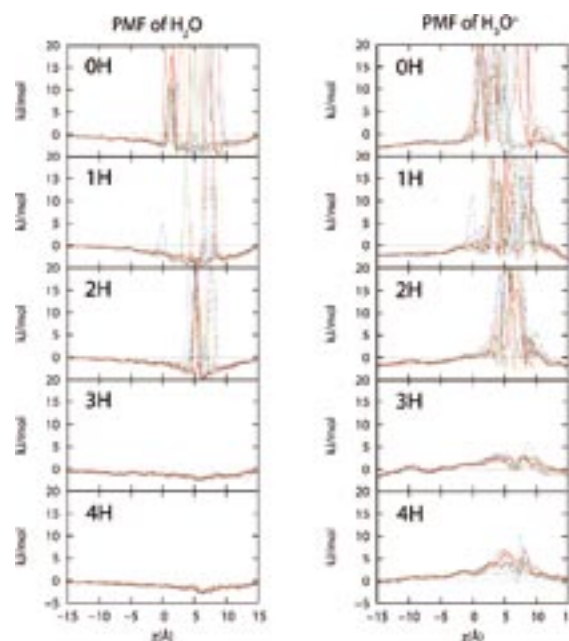


Figure 3. Potential of Mean force of water and hydronium ion in each state, a line represents the PMF for a conformation in the state.

References

- 1) F. Hirata, *Molecular Theory of Solvation*, Kluwer; Dordrecht, Netherlands (2003).
- 2) A. Kovalenko and F. Hirata, *J. Chem. Phys.* **110**, 10095–10112 (1999).
- 3) T. Imai, R. Hiraoka, A. Kovalenko and F. Hirata, *J. Am. Chem. Soc. (Communication)* **127**, 15334–15335 (2005).
- 4) T. Imai, K. Oda, A. Kovalenko, F. Hirata and A. Kidera, *J. Am. Chem. Soc.* **131**, 12430 (2009).
- 5) S. Phongphananee, N. Yoshida and F. Hirata, *J. Phys. Chem. B* **114**, 7967 (2010).
- 6) S. Phongphananee, T. Rungromongkol, N. Yoshida, S. Hannongbua and F. Hirata, *J. Am. Chem. Soc.* **132**, 9782 (2010).

Theory of Photoinduced Phase Transitions

Department of Theoretical and Computational Molecular Science
Division of Theoretical Molecular Science II



YONEMITSU, Kenji
TANAKA, Yasuhiro
KONDO, Naoko

Associate Professor
Assistant Professor
Secretary

Photoirradiation of materials usually creates electrons and holes, which are often accompanied by local structural deformation. With the help of cooperativity, the electronic and/or structural deformation can proliferate to change the physical property such as conductivity, permittivity, and magnetic susceptibility. The resultant nonequilibrium phase may not be reached by changing temperature or pressure because the energy of a photon is much higher than thermal energies. Our theoretical researches are focused on the mechanisms and dynamics of photoinduced phase transitions, how they are controlled, and how the photoinduced electron-lattice states are different from those which are realized in thermal equilibrium.¹⁾

1. Growth Dynamics of Photoinduced Domains in Charge-Ordered Conductors^{2,3)}

We focus on quasi-two-dimensional quarter-filled-band charge-ordered insulators, θ -(BEDT-TTF)₂RbZn(SCN)₄ and α -(BEDT-TTF)₂I₃, where quite different photoinduced melting dynamics are observed. To elucidate such dynamics of initially quite similar, “horizontal-stripe” charge orders, we theoretically study photoinduced evolution of the wave functions in extended Peierls-Hubbard models on anisotropic triangular lattices. The exact many-electron wave function coupled with classical phonons is used for 12-site systems, and the unrestricted Hartree-Fock approximation is used for 144-site systems. These charge orders are stabilized by both Coulomb repulsion and electron-lattice interactions. Their relative importance is different between the two materials.

In θ -(BEDT-TTF)₂RbZn(SCN)₄, the high-temperature metallic phase has a crystal structure with a high symmetry so that different charge-order patterns are nearly degenerate. At low temperatures, a relatively large lattice distortion emerges as molecular rotations (Figure 1, left panel), lifting the degeneracy among these patterns. The lattice stabilization energy is

consequently large, so that a high photoexcitation density is required for the melting. Because each hole-rich stripe is stabilized by uniform molecular rotation, a photoinduced metallic domain created by local photoexcitation grows in a quite anisotropic manner (Figure 2, left panel). The photoinduced charge dynamics shows a complex behavior owing to a large number of nearly degenerate eigenstates.

In α -(BEDT-TTF)₂I₃, the high-temperature metallic phase has a crystal structure with a low symmetry so that charge disproportionation already takes place from kinetic origin. At low temperatures, a small lattice distortion (Figure 1, right panel) is sufficient to stabilize the charge order. The lattice stabilization energy is small, and a low photoexcitation density is sufficient to melt the charge order, producing a metallic phase. Because each hole-rich bond is locally stabilized, a photoinduced metallic domain created by local photoexcitation grows isotropically (Figure 2, right panel), *i.e.*, in any direction of the conducting layer. Thus, a very large metallic domain is finally photogenerated. The photoinduced charge dynamics shows a coherent oscillation when resonantly excited.

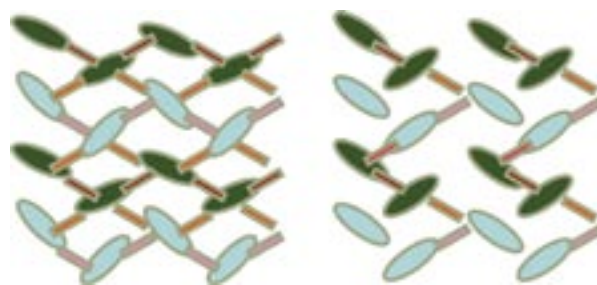


Figure 1. Schematic molecular arrangements in θ -(BEDT-TTF)₂RbZn(SCN)₄ (left) and α -(BEDT-TTF)₂I₃ (right). The ellipses with dark and bright colors represent hole-rich and hole-poor molecules, respectively. Note the angles of ellipses. The rectangles with dark, intermediate, and bright colors correspond to large, intermediate, and small transfer integrals, respectively.

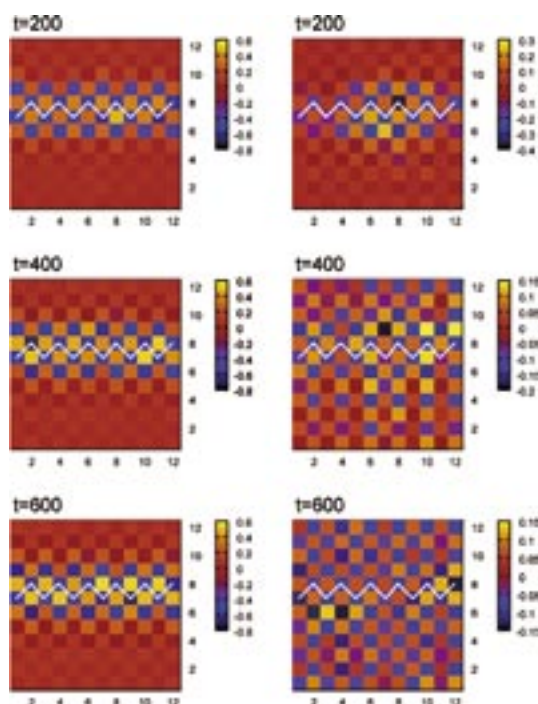


Figure 2. Charge densities at different times, from which those before photoexcitation are subtracted.²⁾ The left and right panels show θ -(BEDT-TTF)₂RbZn(SCN)₄ and α -(BEDT-TTF)₂I₃, respectively. The squares indicate molecules, and the white lines hole-rich stripes.

2. Quantum Electron–Vibration Interference in Photoinduced Insulator–Metal Transition

As described above, a photoinduced insulator-to-metal transition is realized in α -(BEDT-TTF)₂I₃. In reality, the transition is achieved in two stages: An ultrafast one consisting of mainly electronic processes and a slow one consisting of domain processes responsible for the critical slowing down. Although the latter stage can be described in principle by statistical mechanics, the former stage directly reflects interactions among electrons and interactions between electrons and phonons. The latest experimental technique allows us to observe such early-stage dynamics.

Here, it is important to consider electron–molecular-vibration (EMV) couplings. Charge transfers between neighboring molecules are governed by intermolecular transfer integrals. Their magnitudes are about 0.1 or 0.2 eV. The energy range of C=C stretching vibrations inside a molecule is also 0.1 to 0.2 eV. Thus, they can interfere with each other (Figure 3). Then, we theoretically study photoinduced evolution of the wave function in an extended Holstein–Peierls–Hubbard model. The exact many-electron–phonon (molecular vibration) wave function coupled with classical lattice phonons is used for 8-site systems.

Photoexcitation directly oscillates an electron back and forth between neighboring molecules. It excites a molecular

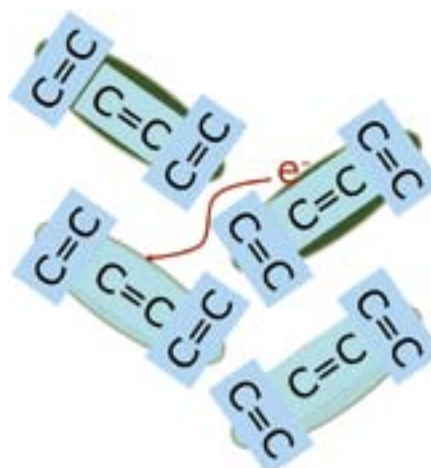


Figure 3. Schematic illustration of electron–molecular-vibration coupling.

vibration through the EMV coupling. They are initially in phase. Soon, their motions become out of phase, causing destructive quantum interference (Figure 4, 50 to 100 fs).

After that, the electronic motion is synchronized with the slower motion of molecular vibrations (Figure 4, after 100 fs) and finally dephased. In reality, there are several modes of molecular vibrations with different energies and coupling strengths. However, the quantum interference obtained above qualitatively simulates the experimentally observed, early-stage dynamics.

From this analysis, the EMV coupling turns out to stabilize the charge order as well as the intersite Coulomb repulsion. The relative importance of molecular vibrations and lattice phonons depends on the timescale of observation. The former is important at the early stage, while the latter is important at the later stage.

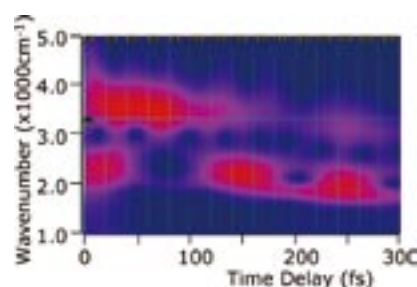


Figure 4. Wavelet transform of photoinduced charge-density modulation.

References

- 1) K. Yonemitsu and K. Nasu, *Phys. Rep.* **465**, 1–60 (2008).
- 2) Y. Tanaka and K. Yonemitsu, *J. Phys. Soc. Jpn.* **79**, 024712 (8 pages) (2010).
- 3) S. Miyashita, Y. Tanaka, S. Iwai and K. Yonemitsu, *J. Phys. Soc. Jpn.* **79**, 034708 (9 pages) (2010).

Theoretical Studies on Condensed Phase Dynamics

Department of Theoretical and Computational Molecular Science
Division of Computational Molecular Science



SAITO, Shinji	Professor
KIM, Kang	Assistant Professor
HIGASHI, Masahiro	IMS Fellow
KOBAYASHI, Chigusa	Post-Doctoral Fellow
YAGASAKI, Takuma	Post-Doctoral Fellow
IMOTO, Sho	Graduate Student*
UENO, Harumi	Secretary

Liquids and biological systems show complicated dynamics because of their structural flexibility and dynamical hierarchy. Understanding these complicated dynamics is indispensable to elucidate chemical reactions and relaxation in solutions and functions of proteins. We have been investigating complex dynamics in supercooled liquids¹⁻³⁾ and chemical reactions in biological systems⁴⁾ using molecular dynamics simulations and electronic structure calculations. In addition, we have been theoretically investigating liquid dynamics by using higher-order nonlinear IR spectroscopy.^{5,6)}

1. Multi-Time Density Correlation Functions in Glass-Forming Liquids: Probing Dynamical Heterogeneity and Its Lifetime¹⁾

A multi-time extension of a density correlation function is introduced to reveal temporal information about dynamical heterogeneity in glass-forming liquids. We utilize a multi-time correlation function that is analogous to the higher-order response function analyzed in multidimensional nonlinear spectroscopy. Here, we provide comprehensive numerical results of the four-point, three-time density correlation function from longtime trajectories generated by molecular dynamics simulations of glass-forming binary soft-sphere mixtures. We confirm that the two-dimensional representations in both time and frequency domains are sensitive to the dynamical heterogeneity and that these reveal the couplings of correlated motions, which exist over a wide range of time scales. The correlated motions detected by the three-time correlation function are divided into mobile and immobile contributions that are determined from the particle displacement during the first time interval. We show that the peak positions of the correlations are in accord with the information on the non-Gaussian parameters of the van Hove self-correlation function. Furthermore, it is demonstrated that the progressive changes in

the second time interval in the three-time correlation function enable us to analyze how correlations in dynamics evolve in time. From this analysis, we evaluated the lifetime of the dynamical heterogeneity and its temperature dependence systematically. Our results show that the lifetime of the dynamical heterogeneity becomes much slower than the α -relaxation time that is determined from the two-point density correlation function when the system is highly supercooled.

2. Slow Dynamics in Random Media: Crossover from Glass to Localization Transition²⁾

We study slow dynamics of particles moving in a matrix of immobile obstacles using molecular-dynamics simulations. The glass transition point decreases drastically as the obstacle density increases. At higher obstacle densities, the dynamics of mobile particles changes qualitatively from glass-like to a Lorentz-gas-like relaxation. This crossover is studied by density correlation functions, nonergodic parameters, mean square displacement, and nonlinear dynamic susceptibility. Our finding is qualitatively consistent with the results of recent numerical and theoretical studies on various spatially heterogeneous systems. Furthermore, we show that slow dynamics is surprisingly rich and sensitive to obstacle configurations. Especially, the reentrant transition is observed for a particular configuration, although its origin is not directly linked to the similar prediction based on the mode-coupling theory.

3. Relation between Conformational Heterogeneity and Reaction Cycle of Ras: Molecular Simulation of Ras⁴⁾

Ras functions as a molecular switch by cycling between the active GTP-bound state and the inactive GDP-bound state.

It is known experimentally that there is another GTP-bound state called state 1. We investigate the conformational changes and fluctuations arising from the difference in the coordinations between the switch regions and ligands in the GTP- and GDP-bound states by using 830 ns molecular dynamics simulations in total. The present result suggests that the large fluctuations among multiple conformations of switch I in state 1 owing to the absence of the coordination between Thr-35 and Mg^{2+} inhibit the binding of Ras to effectors. Furthermore, we elucidate the conformational heterogeneity in Ras by using principal component analysis and propose a two-step reaction path from the GDP-bound state to the active GTP-bound state *via* state 1. The present study suggests that state 1 plays an important role in the signal transduction as an intermediate state of the nucleotide exchange process, though state 1 itself is an inactive state for signal transduction.

4. Molecular Dynamics Simulation of Nonlinear Spectroscopies of Intermolecular Motions in Liquid Water⁵⁾

Water is the most extensively studied of liquids because of both its ubiquity and its anomalous thermodynamic and dynamic properties. The properties of water are dominated by hydrogen bonds and hydrogen bond network rearrangements. Fundamental information on the dynamics of liquid water has been provided by linear infrared (IR), Raman, and neutron-scattering experiments; molecular dynamics simulations have also provided insights. Recently developed higher-order nonlinear spectroscopies open new windows into the study of the hydrogen bond dynamics of liquid water. For example, the vibrational lifetimes of stretches and a bend, intramolecular features of water dynamics, can be accurately measured and are found to be on the femtosecond time scale at room temperature. Higher-order nonlinear spectroscopy is expressed by a multi-time correlation function, whereas traditional linear spectroscopy is given by a one-time correlation function. Thus, nonlinear spectroscopy yields more detailed information on the dynamics of condensed media than linear spectroscopy. In this Account, we describe the theoretical background and methods for calculating higher-order nonlinear spectroscopy; equilibrium and non-equilibrium molecular dynamics simulations, and a combination of both, are used. We also present the intermolecular dynamics of liquid water revealed by fifth-order two-dimensional (2D) Raman spectroscopy and third order IR spectroscopy. 2D Raman spectroscopy is sensitive to couplings between modes; the calculated 2D Raman signal of liquid water shows large anharmonicity in the translational motion and strong coupling between the translational and librational motions. Third-order IR spectroscopy makes it

possible to examine the time-dependent couplings. The 2D IR spectra and three-pulse photon echo peak shift show the fast frequency modulation of the librational motion. A significant effect of the translational motion on the fast frequency modulation of the librational motion is elucidated by introducing the “translation-free” molecular dynamics simulation. The isotropic pump–probe signal and the polarization anisotropy decay show fast transfer of the librational energy to the surrounding water molecules, followed by relaxation to the hot ground state.

5. Ultrafast Energy Relaxation and Anisotropy Decay of the Librational Motion in Liquid Water: A Molecular Dynamics Study⁶⁾

We theoretically investigate intermolecular motions in liquid water in terms of third-order IR spectroscopy. We calculate two-dimensional infrared (2D IR) spectra, pump–probe signals and three-pulse stimulated photon echo signals from the combination of equilibrium and nonequilibrium molecular dynamics simulations. The 2D IR spectra and the three-pulse photon echo peak shift exhibit that the frequency correlation of the librational motion decays with a time scale of 100 fs. The two-color 2D IR spectra and the pump–probe signals reveal that the energy transfer from the librational motion at 700 cm^{-1} to the low frequency motion below 300 cm^{-1} occurs with a time scale of 60 fs and the subsequent relaxation to the hot ground state takes place on a 500 fs time scale. The time scale of the anisotropy decay of the librational motion is found to be ~ 115 fs. The energy dissipation processes are investigated in detail by using the nonequilibrium molecular dynamics simulation in which an electric field pulse is applied. We show that the fast energy transfer from the librational motion to the low frequency motion is mainly due to the librational-librational energy transfer. We also show that the fast anisotropy decay mainly arises from the rapid intermolecular energy transfer.

References

- 1) K. Kim and S. Saito, *J. Chem. Phys.* **133**, 044511 (10 pages) (2010).
- 2) K. Kim, K. Miyazaki and S. Saito, *Europhys. Lett.* **88**, 36002 (5 pages) (2010).
- 3) K. Kim and S. Saito, *J. Phys. Soc. Jpn.* **79**, 093601 (4 pages) (2010).
- 4) C. Kobayashi and S. Saito, *Biophys. J.* **99**, 3726–3734 (2010).
- 5) T. Yagasaki and S. Saito, *Acc. Chem. Res.* **42**, 1250–1258 (2009).
- 6) T. Yagasaki, J. Ono and S. Saito, *J. Chem. Phys.* **131**, 164511 (11 pages) (2009).

* carrying out graduate research on Cooperative Education Program of IMS with Nagoya University

Theoretical Study on Molecular Excited States and Chemical Reactions

Department of Theoretical and Computational Molecular Science
Division of Computational Molecular Science



EHARA, Masahiro
FUKUDA, Ryoichi
TASHIRO, Motomichi
SURAMITR, Songwut
LU, Yun-peng
HORIKAWA, Takenori
KAWAGUCHI, Ritsuko

Professor
Assistant Professor
IMS Research Assistant Professor
Visiting Scientist
Visiting Scientist
Graduate Student
Secretary

Molecules in the excited states show characteristic photo-physical properties and reactivity. We investigate the molecular excited states and chemical reactions which are relevant in chemistry, physics, and chemical biology with developing the highly accurate electronic structure theory. We are also interested in the excited-state dynamics and energy relaxation so that we also develop the methodology of large-scale quantum dynamics. In this report, we report our recent studies on the development of the PCM-SAC-CI method,¹⁾ Molecular double core-hole spectroscopy,²⁾ and Ultraviolet B blocking molecule.³⁾

1. Development of PCM-SAC-CI Method for Solvation Free Energy and Geometry¹⁾

Electronic excitations of molecules and molecular systems in particular circumstances, such as in solutions, have attracted attention for a long time. Solvatochromism, the shift of transition energies by a solvent, is an important consideration in such research. Photochemical and electrochemical reactions in solution are other considerations. Reliable computational studies are essential for elucidating the mechanism of such complex processes because it is difficult to detect short-lived intermediate states in certain solvents experimentally. There is a strong demand for the development of theoretical and computational methods to understand photochemical and electrochemical phenomena in solution, such as those associated with utilizing photo-energy with functional dyes, organic photovoltaic cells, charge transport in batteries and molecular devices, *etc.*

In this work we present the theory and implementation of the symmetry-adapted cluster (SAC) and symmetry-adapted cluster-configuration interaction (SAC-CI) method, including the solvent effect, using the polarizable continuum model (PCM). The PCM and SAC/SAC-CI were consistently combined in terms of the energy functional formalism. The excitation energies were calculated by means of the state-specific approach, the advantage of which over the linear-response approach has been shown. The single point energy calculation and its analytical energy derivatives are presented and imple-

mented, where the free energy and its derivatives are evaluated because of the presence of solute-solvent interactions. We have applied this method to *s-trans* acrolein and methylenecyclopropene of their electronic excitation in solution. The molecular geometries in the ground and excited states were optimized in vacuum and in solution, and both the vertical and adiabatic excitations were studied. The PCM-SAC/SAC-CI reproduced the known trend of the solvent effect on the vertical excitation energies but the shift values were underestimated. The excited state geometry in planar and nonplanar conformations was investigated. The importance of using state-specific methods was shown for the solvent effect on the optimized geometry in the excited state. The mechanism of the solvent effect is discussed in terms of the Mulliken charges and electronic dipole moment.

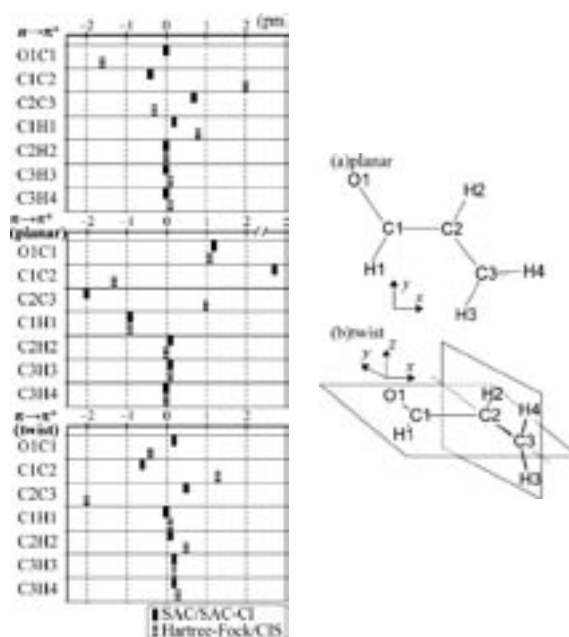


Figure 1. Solvent effect on the changes of bond lengths (in pm) upon electronic excitations for *s-trans* acrolein. The solvent effect denotes the shift in aqueous solution from vacuum.

2. Molecular Double Core-Hole Spectroscopy for Chemical Analysis²⁾

More than two decades ago, Cederbaum *et al.* discovered that the creation of double core vacancies in molecular systems probes the chemical environment more sensitively than the creation of single core vacancies. Two-atomic site double ionization potentials, or briefly two-site DIPs are particularly sensitive to the chemical environment as the examples of the C_2H_2 , C_2H_4 , C_2H_6 and C_6H_6 molecules demonstrate. The chemical shifts of one-atomic site DIPs, or briefly one-site DIPs, were found to be similar to the chemical shifts of the single core level ionization potentials (IPs), or ionization energies (IEs). This finding has given impetus to a number of theoretical studies aimed at elucidating properties of molecular double core hole states.

In this work, we explore the potential of double core hole electron spectroscopy for chemical analysis in terms of x-ray two-photon photoelectron spectroscopy (XTPPS). The creation of deep single and double core vacancies induces significant reorganization of valence electrons. The corresponding relaxation energies and the interatomic relaxation energies are evaluated by CASSCF calculations. We propose a method how to experimentally extract these quantities by the measurement of single and double core-hole ionization potentials (IPs and DIPs). The influence of the chemical environment on these DIPs is also discussed for states with two holes at the same atomic site and states with two holes at two different atomic sites. Electron density difference between the ground and double core-hole states clearly shows the relaxations accompanying the double core-hole ionization. The effect is also compared with the sensitivity of single core hole ionization potentials (IPs) arising in single core hole electron spectroscopy. We have demonstrated the method for a representative set of small molecules LiF, BeO, BF, CO, N_2 , C_2H_2 , C_2H_4 , C_2H_6 , CO_2 and N_2O . The scalar relativistic effect on IPs and on DIPs are briefly addressed.

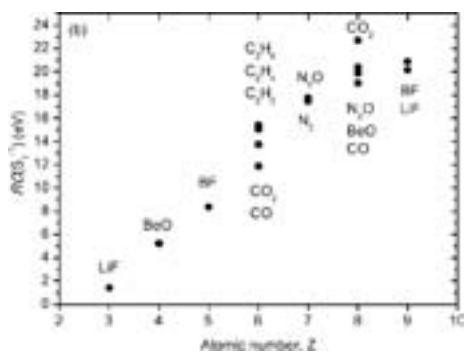


Figure 2. Generalized relaxation energy extracted by the double-core hole IP.

3. Photochemistry of Ultraviolet B Blocking Cinnamates³⁾

We investigated the absorption and emission spectra of UVB blocking cinnamate derivatives with five different substituted positions using the symmetry-adapted cluster configuration interaction (SAC-CI) method. This series included *cis*- and *trans*-isomers of *ortho*-, *meta*-, and *para*-monomethoxy substituted compounds and 2,4,5-(*ortho*-, *meta*-, *para*-) and 2,4,6-(*ortho*-, *para*-) trimethoxy substituted compounds. The ground state and excited state geometries were obtained at the B3LYP and CIS levels of theory. All the compounds were stable as *cis*- and *trans*-isomers in the planar structure in both the S_0 and S_1 states, except the 2,4,6-trimethoxy substituted compound. The SAC-CI calculations reproduced the recently observed absorption and emission spectra satisfactorily. Three low-lying excited states were found to be relevant for the absorption in the UV blocking energy region. The calculated oscillator strengths of the *trans*-isomers were larger than the respective *cis*-isomers, which is in good agreement with the experimental data. In the *ortho*- and *meta*-monomethoxy compounds, the most intense peak was assigned as the transition from next HOMO to LUMO, whereas in the *para*-monomethoxy compound, it was assigned to the HOMO to LUMO transition. This feature was interpreted as being from the variation of the MOs due to the different substituted positions, and was used to explain the behavior of the excited states of the trimethoxy compounds. The emission from the local minimum in the planar structure was calculated for the *cis*- and *trans*-isomers of the five compounds. The relaxation paths which lead to the non-radiative decay were also investigated briefly. Figure 3 compares the UV and SAC-CI spectra of *para*-methoxy-methyl-cinnamate.

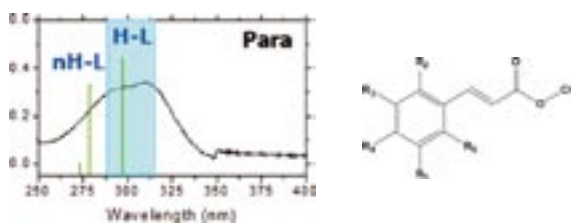


Figure 3. Absorption spectrum of *para*-methoxy-methyl-cinnamate.

References

- 1) R. Cammi, R. Fukuda, M. Ehara and H. Nakatsuji, *J. Chem. Phys.* **133**, 024104 (24 pages) (2010).
- 2) M. Tashiro, M. Ehara, H. Fukuzawa, K. Ueda, C. Buth, N. Z. Kryzhevoi and L. S. Cederbaum, *J. Chem. Phys.* **132**, 184302 (11 pages) (2010).
- 3) M. Promkatkaew, S. Suramitr, T. K. Karpkird, S. Namuangruk, M. Ehara and S. Hannongbua, *J. Chem. Phys.* **131**, 224306 (10 pages) (2009).

Award

EHARA, Masahiro; QSCP (Quantum Systems in Chemistry and Physics) Prize 2009 CMOA (Centre de Mecanique Ondulatoire Appliquee).

Development of New Algorithms for Molecular Dynamics Simulation and Its Application to Biomolecular Systems

Department of Theoretical and Computational Molecular Science
Division of Computational Molecular Science



OKUMURA, Hisashi	Associate Professor
ITOH, G. Satoru	Assistant Professor
KAWAGUCHI, Ritsuko	Secretary
UENO, Harumi	Secretary

Effective samplings in the conformational space by Monte Carlo and molecular dynamics simulations are necessary to predict the native structures of proteins. In the conventional canonical-ensemble simulations, however, it is difficult to realize effective samplings in complex systems such as proteins. This is because the usual canonical-ensemble simulations tend to get trapped in a few of many local-minimum states. To overcome these difficulties, we proposed new generalized-ensemble algorithms.

1. Replica-Exchange Method in van der Waals Radius Space: Overcoming Steric Restrictions for Biomolecules¹⁾

The replica-exchange method is one of the most well-known methods among the generalized-ensemble algorithms. For large systems such as proteins in aqueous solution, however, the usual replica-exchange method has a difficulty. We need to increase the number of replicas in proportion to $O(f^{1/2})$, where f is the number of degrees of freedom. Large biomolecular systems, therefore, require a large number of replicas in the replica-exchange method and hence huge amount of computation time. In order to overcome this difficulty, Hamiltonian replica-exchange method is sometimes employed.

We present a new type of the Hamiltonian replica-exchange method, where the van der Waals radius parameter and not the

temperature is exchanged. By decreasing the van der Waals radii, which control spatial sizes of atoms, this Hamiltonian replica-exchange method overcomes the steric restrictions and energy barriers. Furthermore, the simulation based on this method escapes from the local-minimum free-energy states and realizes effective sampling in the conformational space. We applied this method to an alanine dipeptide (Figure 1) in aqueous solution and showed the effectiveness of the method by comparing the results with those obtained from the conventional canonical and replica-exchange methods.

2. Optimization of Partial Multicanonical Algorithm for Molecular Dynamics and Monte Carlo Simulations

The multicanonical ensemble algorithm is another one of the most well-known generalized-ensemble algorithms. A non-Boltzmann weight factor is employed in this ensemble so that a free one-dimensional random walk can be realized in the potential-energy space. Thus, a simulation with this algorithm can escape from the free-energy-minimum states and sample a wide range of the conformational space. Because of this advantage, the multicanonical algorithm has been frequently applied to a biomolecule, which has a free-energy surface with many local minima. However, the non-Boltzmann weight factor in the multicanonical algorithm is not *a priori* known and has to be determined by a preliminary simulation. As the

system size increases, the distribution of the total potential energy gets narrower. Thus, the determination of the multicanonical weight factor to give a flat distribution becomes difficult in a large system.

In order to alleviate this difficulty, we proposed recently the partial multicanonical ensemble algorithm for molecular dynamics and Monte Carlo simulations. The partial multicanonical algorithm samples a wide range of an important part of the potential energy. Although it is a strong technique for structure prediction of biomolecules, the choice of the partial potential energy has not been optimized. In order to find the best choice, partial multicanonical molecular dynamics simulations of an alanine dipeptide in explicit water solvent were performed with 15 trial choices for the partial potential energy. The best choice was found to be the sum of the electrostatic, Lennard-Jones, and torsion-angle potential energies between solute atoms. In this case, the partial multicanonical simulation sampled all of the local-minimum free-energy states of the P_{II} , C_5 , α_R , α_P , α_L , and C_7^{ax} states and visited these states most frequently. Furthermore, backbone dihedral angles ϕ and ψ rotated very well. It is also found that the most important term among these three terms is the electrostatic potential energy and that the Lennard-Jones term also helps the simulation to overcome the steric restrictions. On the other hand, multicanonical simulation sampled all of the six states, but visited these states less time. Conventional canonical simulation sampled only four of the six states: The P_{II} , C_5 , α_R , and α_P states.

3. Conformational Populations of Ligand-Sized Molecules by Replica Exchange Molecular Dynamics and Temperature Reweighting²⁾

The use of the replica exchange molecular dynamics method for the efficient estimation of conformational populations of ligand-sized molecules in solution is investigated.

We compare the computational efficiency of the traditional constant temperature molecular dynamics technique with that of the parallel replica exchange molecular dynamics method for a series of alkanes and rilpivirine (TMC278), an inhibitor against HIV-1 reverse transcriptase, with implicit solvation. We show that conformational populations are accurately estimated by both methods; however, replica exchange estimates converge at a faster rate, especially for rilpivirine, which is characterized by multiple stable states separated by high-free energy barriers. Furthermore, convergence is enhanced when the weighted histogram analysis method is used to estimate populations from the data collected from multiple replica exchange temperature replicas. For small drug-like molecules with energetic barriers separating the stable states, the use of replica exchange with the weighted histogram analysis method is an efficient computational approach for estimating the contribution of ligand conformational reorganization to binding affinities.

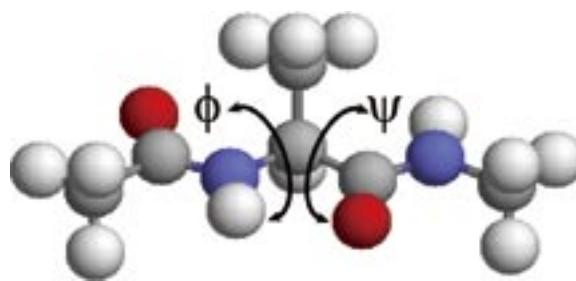


Figure 1. The initial conformations of alanine dipeptide for the molecular dynamics simulation.

References

- 1) S. G. Itoh, H. Okumura and Y. Okamoto, *J. Chem. Phys.* **132**, 134105 (8 pages) (2010).
- 2) H. Okumura, E. Gallicchio and R. M. Levy, *J. Comput. Chem.* **31**, 1357–1367 (2010).

Theory and Computation of Reactions and Properties in Solutions and Liquids

Department of Theoretical and Computational Molecular Science
Division of Computational Molecular Science



ISHIDA, Tateki

Assistant Professor

Our researches are focused on the projects both on ultrafast photoinduced excited state reaction in solution and on ionic liquids (ILs). The project on photoinduced excited state reaction processes in solution focuses on the development of a theoretical method to describe solvent motion and dynamics around a solute molecule in short-time region, including the application of the developed theoretical treatment to solvation processes and excited-state intramolecular electron transfer processes in Betaine dye molecule solution. On the other hand, the aim of ILs projects is to pursue specific interionic dynamics in ILs through many-body polarization effects and to study a new perspective on the characteristics of ILs using dicationic ILs.

1. Photoinduced Excited State Reaction Processes: Effects of Solvent Motions and Solvation Processes on Excited-State Intramolecular Processes in Solution

We propose a procedure for describing equation of motions for atoms considering the inertial term with an interaction site model for capturing solvent dynamics attributed to solvent motions in a short-time regime, $t < 100$ fs. We present a method for calculating the time-dependent evolution of the electronic structure of a solute molecule in solution coupling an electronic structure theory with a solution of the equation which governs the development of the fluctuation of solvent number density with the inertial term. The prescription is applied to the study of solvation dynamics of the simplest betaine dye molecule pyridinium *N*-phenoxide in acetonitrile and methanol in the excited state. It is shown that the coupling between solvation and a fast intramolecular reaction such as charge transfer is likely to play an important role in solvation dynamics of the simplest betaine. Also, it is indicated that intramolecular electron transfer processes in the present dye system could be promoted by solvation dynamics rather than solute structural relaxation such as in twisted intramolecular

charge transfer (TICT) processes.

2. Molecular Dynamics Study of the Dynamical Behavior in Ionic Liquids through Interionic Interactions

We have focused on the interionic dynamics of an IL, 1-Butyl-3-Methylimidazolium cation with the anion, $[\text{PF}_6]^-$, $[\text{BMIm}][\text{PF}_6]$, and have investigated the interionic interaction in the IL and the polarization effects on the system. Molecular dynamics simulations have been carried out to pursue the understanding of interionic properties in ILs at molecular level. The analyses of velocity cross-correlation functions have been performed to study the interionic interactions. We have computed the momentum correlation functions between ionic species. From simulation results, it is suggested that, at the short time region up to 1 ps, the velocity cross-correlation is predominantly governed by the longitudinal contribution. It is found out that, compared with the longitudinal correlation in the nonpolarizable model, the longitudinal motions are further influenced in the polarizable model. It is indicated that the behavior of mean-squared displacement of the cation at a long-time region is not influenced by polarization effects, while the anion shows important difference. Also, it is concluded that the cage effect in ILs could be reduced by many-body polarization effects. (DOI 10.1016/j.jnoncrysol.2010.05.086)

3. New Perspective on the Characteristics of Ionic Liquids

We focus on dicationic ILs with typical counter anions. The molecular dynamics simulations for dicationic ILs systems have been performed. The interionic interactions and the properties dependent on the specific distribution of ionic species are investigated including the analysis of velocity autocorrelation and polarizability time correlation functions.

Visiting Professors



Visiting Professor
NAKAI, Hiromi (*from Waseda University*)

Linear-Scaling Divide-and-Conquer Correlation Theory for Treating Large Systems

“Divide each of the difficulties under examination into as many parts as possible, and as might be necessary for its adequate solution.” This quote is from René Descartes, the famous French philosopher regarded as a founder of modern philosophy, in his “Discourse on Method.” This phrase is none other than the first statement of the divide-and-conquer (DC) approach. The importance of this philosophy has been universal among almost all sciences, especially computer science. The conventional correlation calculation posed difficulties with large systems due to its unfavorable scaling of computational costs. Nakai *et al.* have presented a breakthrough in correlation calculations by combining the DC method with energy density analysis (EDA). The DC-correlation method is capable of achieving linear scaling of CPU times with respect to system size. This success will open new vistas for computational chemistry across a wide range of scientific and technological fields, nanomaterials and biosystems among them.



Visiting Professor
TANIMURA, Yoshitaka (*from Kyoto University*)

Modeling, Calculating, and Analyzing Multidimensional Spectroscopies

Spectral line shapes in a condensed phase contain information from various dynamic processes that modulate the transition energy, such as microscopic dynamics, inter- and intra-molecular couplings, and solvent dynamics. In multidimensional spectroscopy, the nonlinear response functions of a molecular dipole or polarizability are measured using ultra-short pulses to monitor inter- and intra-molecular vibrational motions. Because complex profile of such signal depends on the many dynamic and structural aspects of molecular system, researchers would like to have a theoretical understanding of these phenomena. We explore and describe the roles of different physical phenomena that arise from the peculiarities of the system-bath coupling in multidimensional spectra. Using the hierarchy formalism, we precisely calculate multi-dimensional spectra for a single and multi-mode anharmonic system for inter- and intra-molecular vibrational modes.



Visiting Associate Professor
NISHIYAMA, Katsura (*from Shimane University*)

Elucidation of Primary Photochemical Processes of Nanoscaled Luminescent Devices

We have synthesized nanoscaled structures likewise nanorods, nanotubes, and nanowires with a skeleton of rare earth elements. To drive luminescent functions from nanostructures produced in our group, we introduce “light-harvesting antennas” having organic/rare earth hybridized structures into the nano skeleton. Along with the experimental projects, our group has also carried out theoretical studies for the elucidation of primary photochemical processes in the condensed phase. For instance, the RISM framework incorporated with theories describing time evolution of the system has been employed to obtain molecular view of solvation dynamics. Recently we undertake to describe initial luminescent processes using the RISM theory together with quantum chemical approaches.